Journal of Computational Applied Mechanics 2024, 55(3): 423-439

DOI: 10.22059/JCAMECH.2024.376625.1096

RESEARCH PAPER

Numerical investigation on unsteady compressible flow of viscous fluid with convection under the effect of Joule heating

S. Zafar [a], Ambreen A Khan [a], Sadiq M Sait [b,c], R. Ellahi [a, d,*]

[a] *Department of Mathematics & Statistics, International Islamic University, Islamabad-4400, Pakistan*
[b] *Department of Computer Engineering, King Fahd University of Petroleum & Minerals, Dhahran-31261, Saudi Arabia*
[c] *Interdisciplinary Research Center for Smart Mobility and Logistics, King Fahd University of Petroleum & Minerals, Dhahran-3126, Saudi Arabia*
[d] *Center for Modeling & Computer Simulation, Research Institute, King Fahd University of Petroleum & Minerals, Dhahran-31261, Saudi Arabia*

Abstract

The study of compressible flow plays a fundamental role in the design of heat exchangers at high temperature and pressure. Compressible flow is used to design the aerodynamic structure, engines, and high-speed vehicles. In view of these utilities, this paper is deliberated to acquire the analysis of the unsteady compressible flow of a viscous fluid through an inclined asymmetric channel with thermal effects. Special attention is paid to convective heat transfer with impact of viscous dissipation, source/sink, and joule heating effects. In addition, thermal flow is analyzed through slip boundary conditions. The current problem is modeled through the laws of energy, momentum, and mass with the help of a fluid's response towards compression. As a result, the coupled nonlinear partial differential equations are obtained, which are investigated through a well-known numerical approach, the explicit finite difference method. The study examines impact of several parameters on the flow rate, velocity, and temperature with the help of graphical representations. The behavior of flow rate is intended to change with time.

Keywords: Compressible flow, Convective heat transfer, Joule heating, Source, Sink; Finite difference method

1. Introduction

Peristalsis refers to the propagation of waves of pressure or fluid movement that help transport liquids or gases through the system. Peristalsis can also occur in fluid-filled structures, such as in certain types of tubes or vessels within the body or in engineered systems. In industrial and engineering applications, peristalsis can be replicated or utilized to pump fluids through flexible tubing without the need for internal moving parts. Peristaltic pumps work by compressing and relaxing the tubing in a rhythmic fashion, creating waves of pressure that push fluid through the system. The pioneers of the peristaltic study are Latham [1] and Shapiro et al. [2]. There are a lot of applications of peristaltic flow in various fields. The peristaltic flow of viscous incompressible fluid is debated by Elshehawey et al.

* Corresponding author, (R. Ellahi): E-mails: rellahi@alumni.ucr.edu; rahmatellahi@yahoo.com

[3]. The peristaltic flow of second order fluid in a tube is described by Siddique et al. [4]. The peristaltic motion of non-Newtonian liquid is discussed by Vaidya et al. [5] through an inclined tube. The peristaltic study of Maxwell liquid flow is explored by Hina et al. [6] in an asymmetric channel. The introduction of asymmetric wave propagation is given by Taylor [7]. Furthermore, peristaltic mechanism of wave is more developed in an asymmetric channel, is explored by Eytan and Elad [8] as an application in intra uterine liquid flow in a nonpregnant uterus. A few recent researches on different asymmetric channels are listed in [9-11].

A numerical method naming finite difference technique is used to estimate the solutions of differential equations, especially partial differential equations (PDEs). This approach has a lot of applications in computational fluid dynamics, engineering, finance, and physics, among others. The behavior of viscous, unsteady, and incompressible fluid flow is analyzed by finite difference method [12]. A numerical approach named implicit finite difference simulations in an asymmetric channel of a biconvective flow of nanofluid is described by Abbasi et al. [13]. Hayat et al. [14] deliberated the impact of nanomaterials with viscous dissipation and melting heat by the finite difference method. Reza et al. [15] observed the behavior of unsteady MHD flow in Casson fluid that passed a stretching surface by using the explicit finite difference technique. Some updated literature on this analysis is expressed in [13, 16].

The phenomenon of convective heat transfer has received particular attention in addition to magnetic field with inclination. It is impossible to dispute the importance of convective heat transfer rate in high temperature processes. Applications such as gas turbines, thermal energy storage, and nuclear power plants are able to utilize these processes. Different parts of the human body are treated through heat emission. Using this method, the damaged portions of the body's blood vessels are directly heated. Among other things, it serves to treat persistent muscular shortening, muscle spasms, and chronic wide-spread irritation. There are notable papers relevant to the topic under investigation [17-26] available in existing literature.

A compressible fluid is one whose density is variable. A fluid that flows at variable pressure, temperature, and velocity and causes significant changes in the fluid's density is said to be compressible flow. The knowledge for compressed air flow is employed in many natural and technological processes. Aarts and Ooms [27] were pioneers for the study of compressible flows and examined how ultrasonic radiation affected the flow of compressible fluid in porous media. The MHD effect and porosity on compressible Maxwell fluid is examined by Mekheimer et al. [28], who investigated lower flow rate for the Newtonian fluid relative to the non-Newtonian fluid.

According to the literature cited above, there is a lot of discussion given about the peristaltic flow of compressible fluid in symmetric and asymmetric channels. However, no work is done on the unsteady convective peristaltic flow of compressible fluid in an inclined channel with the effect of source/sink and joule heating. The joule heating and source/sink may have inferences for heat transfer systems and energy conversion. This article reveals thermal analysis of an unsteady compressible flow of viscous fluid with the effects of source/sink and joule heating in an inclined channel. A finite difference method is implemented to examine the above problem. This study also described the flow rate.

2. Mathematical Modelling

An electrically conducting compressible flow of viscous fluid in a 2D asymmetric inclined channel of width $b_1 + b_2$ with (x, y) as coordinate axis. The fluid constitutes an effect of magnetic field acting perpendicular to the channel in the presence of source/sink. Heat transfer analysis is also employed with thermal buoyancy effect and viscous dissipation. Moreover, joule heating effect is also present. The sinusoidal waves are moving with speed c along the walls of the channel. Fluid flow is due to propagation of these sinusoidal waves.

Mathematically, wave propagating through channel walls are described as:

$$H_1(x,t) = +b_1 + a_1 cos\left(\frac{2\pi}{\lambda}(x - ct)\right) = +b_1 + \eta_1, \qquad \text{Upper Wall} \tag{1}$$

$$H_2(x,t) = -b_2 - a_2 cos\left(\frac{2\pi}{\lambda}(x - ct) + \phi\right) = -b_2 - \eta_2, \qquad \text{Lower Wall} \tag{2}$$

where a_1, a_2 are waves amplitude and η_1, η_2 are vertical displacement from mean position d_1 and d_2 respectively. Wavelength and phase difference are denoted by λ and ϕ, respectively.

Moreover, a_1, a_2, b_1, b_2 and ϕ obeys the following inequality;

$$a_1^2 + a_2^2 + 2a_1a_2 cos\phi \leq (b_1 + b_2)^2.$$

Flow's governing equations are as follows:

Conservation of mass

$$\rho_t + (\boldsymbol{V}.\nabla\rho) + \rho(\nabla.\boldsymbol{V}) = 0. \quad (3)$$

Conservation of momentum

$$\rho V_t + \rho(\boldsymbol{V}.\boldsymbol{\nabla})\boldsymbol{V} = -\boldsymbol{\nabla}p + \boldsymbol{\nabla}.\boldsymbol{S} + \boldsymbol{J}\times\boldsymbol{B} + \rho\boldsymbol{b_f}(T - T_0). \quad (4)$$

Energy equation

$$\rho C_p(T_t + (\boldsymbol{V}.\boldsymbol{\nabla})T) = p_t + (\boldsymbol{V}.\boldsymbol{\nabla})p + k\nabla^2 T + \boldsymbol{J}.\boldsymbol{J} + \varphi + Q_0, \quad (5)$$

where p, C_p, ξ, ρ, μ, t, $\boldsymbol{V}$, k, and T_0 represents pressure, specific heat, coefficient of thermal expansion, density, dynamic viscosity, time, velocity vector, thermal conductivity and temperature of lower wall, respectively.

Extra stress tensor S is defined as:

$$S = \mu(\boldsymbol{L} + \boldsymbol{L}^T - \tfrac{2}{3}(\boldsymbol{\nabla}.\boldsymbol{V})), \quad (6)$$

where $\boldsymbol{L}$ the velocity gradient and $\boldsymbol{L}^T$ is its transpose.

$\boldsymbol{J}$ represents the current density and is described as

$$\boldsymbol{J} = \sigma(\boldsymbol{V}\times\boldsymbol{B}). \quad (7)$$

where σ denotes the fluid electric conductivity.

Also, viscous dissipation is defined as

$$\varphi = \mu\left[2{u_x}^2 + 2{v_y}^2 + (u_y + v_x)^2 - \tfrac{2}{3}(u_x + v_y)^2\right]. \quad (8)$$

The ideal state equation, which characterizes the fluid reaction, is provided as

$$\frac{1}{\rho}\frac{\partial\rho}{\partial p} = k_c, \quad (9)$$

with the solution

$$\rho = \rho_0 exp\big(k_c(p - p_c)\big), \quad (10)$$

where, k_c the fluid's compressibility and ρ_0 the density at the reference pressure p_c.

The leading equations will take the form with above mentioned assumptions

$$\rho_t + u\rho_x + v\rho_y + \rho(u_x + v_y) = 0 \quad (11)$$

.

$$\rho\big(u_t + uu_x + vu_y\big) = -p_x + \mu\left(\nabla^2 u + \tfrac{1}{3}\frac{\partial}{\partial x}\big(u_x + v_y\big)\right) - \sigma u B_0^2 + \rho g(T - T_0)\xi sin\alpha,$$

(12)

$$\rho\big(v_t + uv_x + vv_y\big) = -p_y + \mu\left(\nabla^2 v + \tfrac{1}{3}\frac{\partial}{\partial y}\big(u_x + v_y\big)\right) - \rho g(T - T_0)\xi cos\alpha, \quad (13)$$

$$\rho C_p\big(T_t + uT_x + vT_y\big) = p_t + up_x + vp_y + k\nabla^2 T + \sigma u^2 B_0^2 + \varphi + Q_0. \quad (14)$$

Eq. (11) takes the form after using Eq. (10)

$$k_c\big(p_t + up_x + vp_y\big) + \big(u_x + v_y\big) = 0. \quad (15)$$

The boundary conditions are

At $t = 0, u = 0, T = 0.$

Horizontal velocity is described with slip condition, i.e.,

$$u = \begin{cases} -Au_y \\ Au_y \end{cases}, \quad \text{at } y = \begin{cases} H_1 \\ H_2 \end{cases}. \quad (16)$$

Vertical velocity is deliberated with no permeability, i.e.,

$$v = \begin{cases} \eta_{1t} \\ \eta_{2t} \end{cases}, \quad \text{at} \quad y = \begin{cases} H_1 \\ H_2 \end{cases}. \tag{17}$$

Thermal slip condition, i.e.,

$$T \pm \beta_1 T_y = \begin{cases} T_0 \\ T_1 \end{cases}, \text{ at } y = \begin{cases} H_1 \\ H_2 \end{cases}. \tag{18}$$

Introduce the following non-dimensional variables which are to be defined as

$$\theta = \frac{T-T_0}{T_1-T_0}, \ \eta' = \frac{\eta}{b}, u' = \frac{u}{c}, v' = \frac{v}{c}, \ \rho' = \frac{\rho}{\rho^0}, t' = \frac{ct}{b_1}, \ \epsilon = \frac{a_1}{b_1}, p' = \frac{p}{\rho^0 c^2}, \ x' = \frac{x}{b_1}, \ h_1 = \frac{H_1}{b_1},$$

$$h_2 = \frac{H_2}{b_2}, b = \frac{b_2}{b_1}, y' = \frac{y}{b_1}, h_2 = \frac{H_2}{b_2}, a = \frac{a_2}{a_1}, p_c{}' = \frac{p_c}{\rho^0 c^2}, \alpha = \frac{2\pi b_1}{\lambda}, K_n = \frac{A}{b_1}, \chi = k_c \rho_0 c^2, Ma = \frac{c}{a},$$

$$Re = \frac{\rho_0 c b_1}{\mu}, H = \frac{\sigma B_0^2 b_1}{\rho_0 c}, \ Pr = \frac{\mu C_p}{k}, S_{ij}' = \frac{b_1}{\mu c} S_{ij}, \varphi' = \frac{b^2 \varphi}{c^2 \mu}, \xi = \frac{1}{T_1 - T_0} \frac{\nabla \rho}{\rho}, Gr = \frac{b_1^3 g}{v_0^2} \frac{\nabla \rho}{\rho}, \Omega = \frac{Q_0 b_1^2}{k(T_1 - T_0)}.$$

(19)

In terms of Eqs. (19), Eqs. (11-14) and (16-18) reduces to

$$\chi\left(p_t + up_x + vp_y\right) + u_x + v_y = 0, \tag{20}$$

$$\rho\left(u_t + uu_x + vu_y\right) = -p_x + \frac{1}{Re}\left[\frac{4}{3}u_{xx} + \frac{1}{3}v_{xy} + u_{yy}\right] - Hu + \frac{\rho sin\alpha\theta Gr}{Re}, \tag{21}$$

$$\rho\left(v_t + uv_x + vv_y\right) = -p_y + \frac{1}{R}\left[v_{xx} + \frac{4}{3}u_{yy} + \frac{1}{3}u_{xy}\right] + \frac{\rho cos\alpha\theta Gr}{Re}, \tag{22}$$

$$\rho\left(\theta_t + u\theta_x + v\theta_y\right) = (\gamma^* - 1)Ma^2\left[p_t + up_x + vp_y\right] + \frac{1}{Re\ Pr}\left[\theta_{xx} + \theta_{yy}\right] + \frac{Ma^2(\gamma^*-1)}{R}\left[2(u_x)^2 + \left(u_y + v_x\right)^2 + 2\left(v_y\right)^2 - \frac{2}{3}\left(v_y + u_x\right)^2\right] + HMa^2(\gamma^* - 1)u^2 + \frac{\Omega}{RePr}, \tag{23}$$

$$\eta_1(x,t) = \epsilon \cos\left(\alpha(x-t)\right), \tag{24}$$

$$\eta_2(x,t) = \epsilon \cos(\alpha(x-t) + \phi), \tag{25}$$

At

$$y = \begin{cases} h_1 = 1 + \eta_1 \\ h_2 = -b - \eta_2 \end{cases}; \tag{26}$$

$$u = \begin{cases} -K_n u_y \\ K_n u_y \end{cases}, \quad v = \begin{cases} \eta_{1t} \\ -\eta_{2t} \end{cases}, \quad \theta \pm \beta_1 \theta_y = \begin{cases} 0 \\ 1 \end{cases}. \tag{27}$$

3. Numerical Technique

In order to calculate the solution, an explicit finite difference method is applied. Finite difference method converts coupled current problem from the set of nonlinear PDEs along with boundary conditions. Space variables and time variables are approximated by the central and forward differences in this present study. We denote $u(x_k, y_s, t_n)$ as $u_{k,s}^n$. Using this method, one may estimate partial derivatives of u as follows:

$$u_t = \left(\frac{u_{k,s}^{n+1} - u_{k,s}^n}{\Delta t}\right), u_x = \left(\frac{-u_{k-1,s}^n + u_{k+1,s}^n}{2\Delta x}\right), u_y = \left(\frac{-u_{k,s-1}^n + u_{k,s+1}^n}{2\Delta y}\right), \tag{28}$$

$$u_{xx} = \left(\frac{u_{k-1,s}^n - 2u_{k,s}^n + u_{k+1,s}^n}{(\Delta x)^2}\right), \ u_{yy} = \left(\frac{u_{k,s-1}^n - 2u_{k,s}^n + u_{k,s+1}^n}{(\Delta y)^2}\right), \tag{29}$$

$$u_{xy} = \left(\frac{u^n_{k-1,s-1} - u^n_{k+1,s-1} - u^n_{k-1,s+1} + u^n_{k+1,s+1}}{4(\Delta x)(\Delta y)}\right). \tag{30}$$

When v and θ are replaced by u in the partial derivatives of finite difference technique, getting into the approximations for finite difference technique in Eqs. (28-30), respectively. Using these approximations into Eqs. (20-27) are given as

$$p^{n+1}_{k,s} = p^n_{k,s} - \Delta t\left[u^n_{k,s}\left(\frac{p^n_{k+1,s} - p^n_{k-1,s}}{2\Delta x}\right) + \left(\frac{-p^n_{k,s-1} + p^n_{k,s+1}}{2\Delta y}\right)v^n_{k,s} + \left(\frac{u^n_{k+1,s} - u^n_{k-1,s}}{2\chi\Delta x}\right) + \left(\frac{v^n_{k,s+1} - v^n_{k,s-1}}{2\chi\Delta y}\right)\right], \tag{31}$$

$$u^{n+1}_{k,s} = u^n_{k,s} - \Delta t\left[u^n_{k,s}\left(\frac{u^n_{k+1,s} - u^n_{k-1,s}}{2\Delta x}\right) + v^n_{k,s}\left(\frac{u^n_{k,s+1} - u^n_{k,s-1}}{2\Delta y}\right) + \frac{1}{exp[\chi(p^n_{k,s} - p_c)]}\left\{\left(\frac{p^n_{k+1,s} - p^n_{k-1,s}}{2\Delta x}\right) - \frac{1}{Re}\left[\frac{4}{3}\left(\frac{u^n_{k+1,s} - 2u^n_{k,s} + u^n_{k-1,s}}{(\Delta x)^2}\right) + \left(\frac{u^n_{k,s+1} - 2u^n_{k,s} + u^n_{k,s-1}}{(\Delta y)^2}\right) + \frac{1}{3}\left(\frac{v^n_{k-1,s-1} + v^n_{k+1,s+1} - v^n_{k-1,s+1} - v^n_{k+1,s-1}}{4(\Delta x)(\Delta y)}\right)\right] + Mu^n_{k,s}\right\} - \frac{exp[\chi(p^n_{k,s} - p_c)]Gr\sin\alpha\theta^n_{k,s}}{Re}\right], \tag{32}$$

$$v^{n+1}_{k,s} = v^n_{k,s} - \Delta t\left[u^n_{k,s}\left(\frac{v^n_{k+1,s} - v^n_{k-1,s}}{2\Delta x}\right) + v^n_{k,s}\left(\frac{v^n_{k,s+1} - v^n_{k,s-1}}{2\Delta y}\right) + \frac{1}{exp[\chi(p^n_{k,s} - p_c)]}\left\{\left(\frac{p^n_{k,s+1} - p^n_{k,s-1}}{2\Delta y}\right) - \frac{1}{Re}\left[\left(\frac{-2v^n_{k,s} + v^n_{k+1,s} + v^n_{k-1,s}}{(\Delta x)^2}\right) + \frac{1}{3}\left(\frac{u^n_{k+1,s+1} - u^n_{k+1,s-1} + u^n_{k-1,s-1} - u^n_{k-1,s+1}}{4(\Delta x)(\Delta y)}\right) + \frac{4}{3}\left(\frac{v^n_{k,s+1} - 2v^n_{k,s} + v^n_{k,s-1}}{(\Delta y)^2}\right)\right] - \frac{exp[\chi(p^n_{k,s} - p_c)]Gr\cos\theta^n_{k,s}}{Re}\right\}\right], \tag{33}$$

$$\theta^{n+1}_{k,s} = \theta^n_{k,s} - \Delta t\left[u^n_{k,s}\left(\frac{\theta^n_{k+1,s} - \theta^n_{k-1,s}}{2\Delta x}\right) + v^n_{k,s}\left(\frac{\theta^n_{k,s+1} - \theta^n_{k,s-1}}{2\Delta y}\right) - \frac{1}{exp[\chi(p^n_{k,s} - p_c)]}\left[(\gamma^* - 1)Ma^2\left[u^n_{k,s}\left(\frac{p^n_{k+1,s} - p^n_{k-1,s}}{2\Delta x}\right) + v^n_{k,s}\left(\frac{p^n_{k,s+1} - p^n_{k,s-1}}{2\Delta y}\right) + \left(\frac{p^{n+1}_{k,s} - p^n_{k,s}}{\Delta t}\right)\right] + \left[\left(\frac{\theta^n_{k+1,s} - 2\theta^n_{k,s} + \theta^n_{k-1,s}}{(\Delta x)^2}\right) + \left(\frac{\theta^n_{k,s+1} - 2\theta^n_{k,s} + \theta^n_{k,s-1}}{(\Delta y)^2}\right)\right]\frac{1}{Pr.Re} + \frac{(\gamma^* - 1)Ma^2}{Re}\left[2\left(\frac{-v^n_{k,s-1} + v^n_{k,s+1}}{2\Delta y}\right)^2 + 2\left(\frac{-u^n_{k-1,s} + u^n_{k+1,s}}{2\Delta x}\right)^2 + \left[\left(\frac{v^n_{k+1,s} - v^n_{k-1,s}}{2\Delta x}\right) + \left(\frac{u^n_{k,s+1} - u^n_{k,s-1}}{2\Delta y}\right)\right]^2 - \frac{2}{3}\left[\left(\frac{u^n_{k+1,s} - u^n_{k-1,s}}{2\Delta x}\right) + \left(\frac{-v^n_{k,s-1} + v^n_{k,s+1}}{2\Delta y}\right)\right]^2\right] - HMa^2(\gamma^* - 1)(u^n_{k,s})^2 - \frac{\Omega}{RePr}\right]\right]. \tag{34}$$

$$At\ t = 0,\ \ u^n_{k,s} = 0,\ \ v^n_{k,s} = 0,\ \ \theta^n_{k,s} = 0, \tag{35}$$

At

$$y = \begin{cases} h_1 = 1 + \eta_1 \\ h_2 = -b - \eta_2 \end{cases};\qquad u^n_{k,s} = \begin{cases} -K_n\left(\frac{u^n_{k,s+1} - u^n_{k,s-1}}{2\Delta y}\right) \\ K_n\left(\frac{u^n_{k,s+1} - u^n_{k,s-1}}{2\Delta y}\right) \end{cases},\qquad v^n_{k,s} = \begin{cases} \left(\frac{(\eta_1)^{n+1}_{k,s} - (\eta_1)^n_{k,s}}{\Delta t}\right) \\ -\left(\frac{(\eta_2)^{n+1}_{k,s} - (\eta_2)^n_{k,s}}{\Delta t}\right) \end{cases},$$

$$\theta^n_{k,s} \pm \beta_1\left(\frac{\theta^n_{k,s+1} - \theta^n_{k,s-1}}{2\Delta y}\right) = \begin{cases} 0 \\ 1 \end{cases}. \tag{36}$$

4. Discussion

This section includes a detailed graphical discussion of axial velocity variation, flow rate, and temperature against sundry parameters in order to make a quantitative assessment of the under discussed parameters in the current study. We repeatedly executed our code with different common parameters. The parameters, which are kept constant throughout the whole study: $\epsilon = 0.5,\ p_c = 10,\ K_n = 0.01,\ d = 1.5,\ \Omega = 0.5$.

Figures 1-8 examined the impact of different parameters like $R, \phi, M, a, \chi, Gr, \Omega$(source and sink) on axial velocity. Figure 1 illustrates the impact of Reynolds number on axial velocity. It is explored that axial velocity is decreasing near the lower wall of channel and increasing near the upper wall of channel; however, axial velocity is constant at center of channel. Figure 2 displays the impact of phase difference on velocity. It has been seen that axial velocity is increasing with the increment in ϕ near the lower wall of channel and remains constant at the upper wall of channel. Figure 3 portrays the impact of magnetic field on velocity of fluid. It is deliberated that velocity of fluid slows down as the magnetic number increases as a result of the magnetic field's resistance. Figure 4 explores the impact of wall amplitude a against axial velocity. It is evident that axial velocity shows increment as wall amplitude is increased. Figure 5 explains to the behavior of compressibility parameter on axial velocity. It is explored that the velocity increasing in the vicinity of the walls by increment in compressibility parameter. Figure 6 illustrates the impact of Grashof number on fluid velocity. It is examined that there are buoyancy forces dominants inside the channel so fluids velocity is increased by increasing Grashof number. Figures 7 and 8 shows the impact of source and sink parameter against fluid velocity. It is clear from the graphical view that there is an increasing behavior of velocity of fluid as source parameter increases as compared to sink parameter, fluid velocity decreases.

Figures 9-15 explain the behavior of sundry parameters, like $a, M, Gr, Pr, Ma, R, \phi$ on dimensionless temperature. Figure 9 explores the behavior of wall amplitude on temperature. As wall amplitude increases the temperature of the fluid slows down. Figure 10 examines the impact of magnetic number relative to the phase difference on dimensionless temperature. As the magnetic number and phase difference increase, there is an increase in the temperature of the fluid. Figure 11 portrays the impact of Grashof number on the temperature of the fluid. It has been seen that there is an oscillatory behavior of temperature against Grashof number, at the upper wall there is maximum temperature while at the lower wall of channel the temperature is minimum. Figure 12 examines that the impact of Prandtl number on temperature. As the behavior of temperature is oscillatory at the near of upper wall there is greater momentum diffusivity, while at the lower wall of the channel there is thermal diffusivity. Figure 13 deliberates the impact of temperature against Mach number. The temperature of the fluid increases as the Mach number increases. The influence of temperature profile is visualized against the Reynolds number in Figure 14. There is an oscillatory behavior of the temperature of fluid at the near of upper wall there is decrement in the temperature while at the upper wall there is an increment in fluid's temperature. Figure 15 depicts the impact of phase difference on temperature. It has been seen that temperature of the fluid increases as the phase difference increases.

Figures 16-18 show the flow rate for M, R, and χ. It is explored that Reynolds number enhances the fluid flow because there are inertial forces as a dominant factor in figure 16. Figure 17 shows the impact of magnetic number on flow rate of fluid. When there is a higher magnetic field present, fluids require more force to maintain the same flow rate. Therefore, a decrease in flow rate results from an increase in the magnetic number. Figure 18 deliberated the behavior of compressibility parameter χ on flow rate. There is decrement in flow rate with an increment in the compressibility parameter of fluid.

5. Conclusions

In this section, this article investigates the thermal analysis of peristaltic flow of unsteady compressible fluid under the effect of viscous dissipation. The imitation of Joule heating effect with source/sink is also incorporated. The notable detection of the above analysis is given and outlined as follow:

- Fluid velocity is enhanced by the compressibility parameter, and in this way, fluid moves faster.
- The effect of inertial forces shows an oscillatory response towards axial velocity while the impact of buoyancy forces enhances the fluid flow against axial velocity.
- The resistive nature of magnetic field slows down for axial velocity.

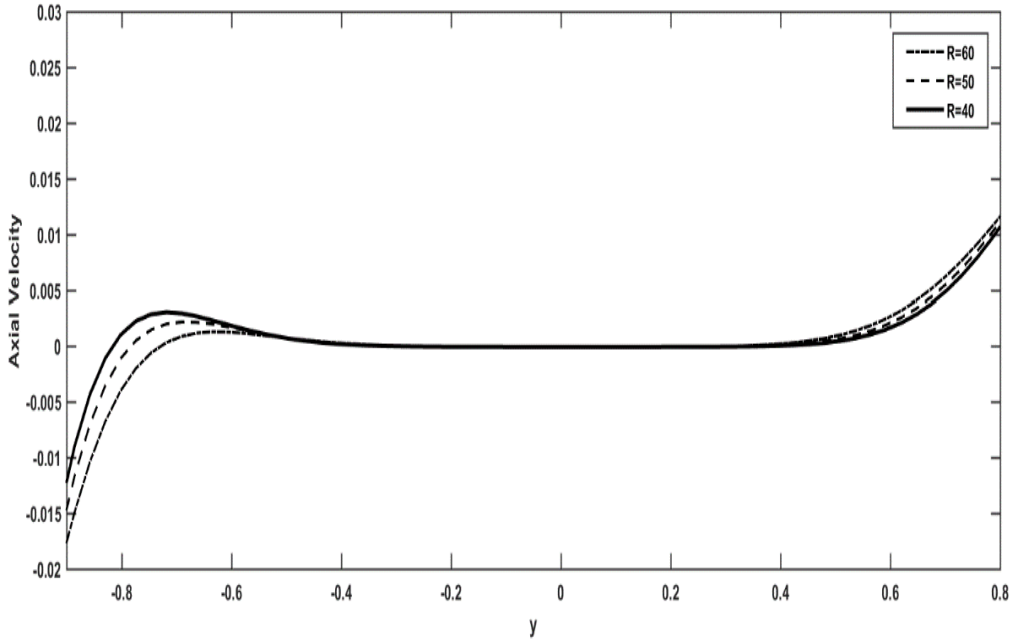

Fig. 1: Axial velocity for R for $\alpha = 0.62,\ Ma = 0.3,\ Pr = 7.56, d = 1.5, M = 0.2$.

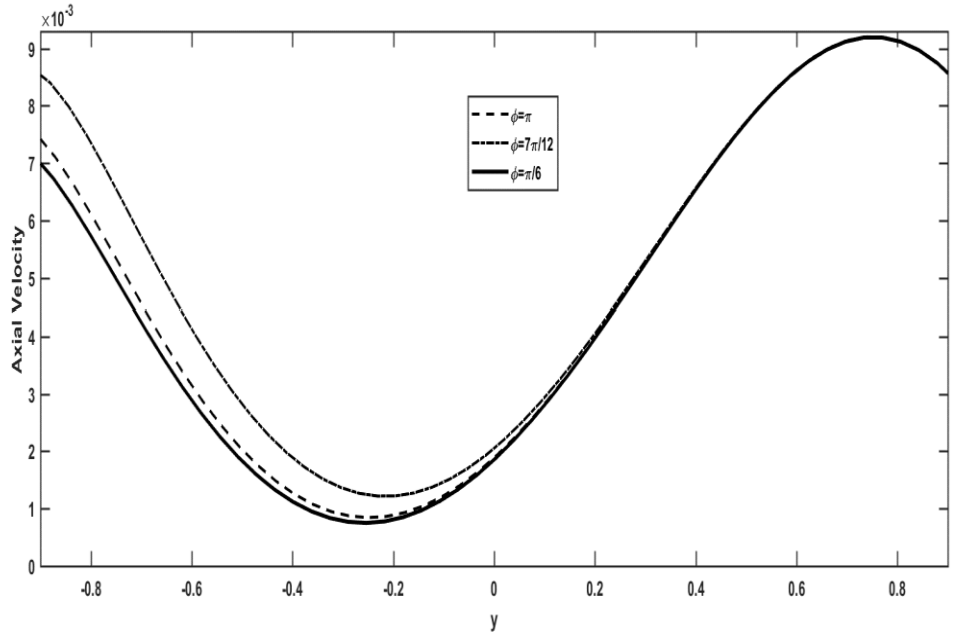

Fig. 2: Axial velocity for ϕ for $Pr = 7.56, M = 0.9, d = 1.5, Ma = 0.3,\ \alpha = 0.5,$.

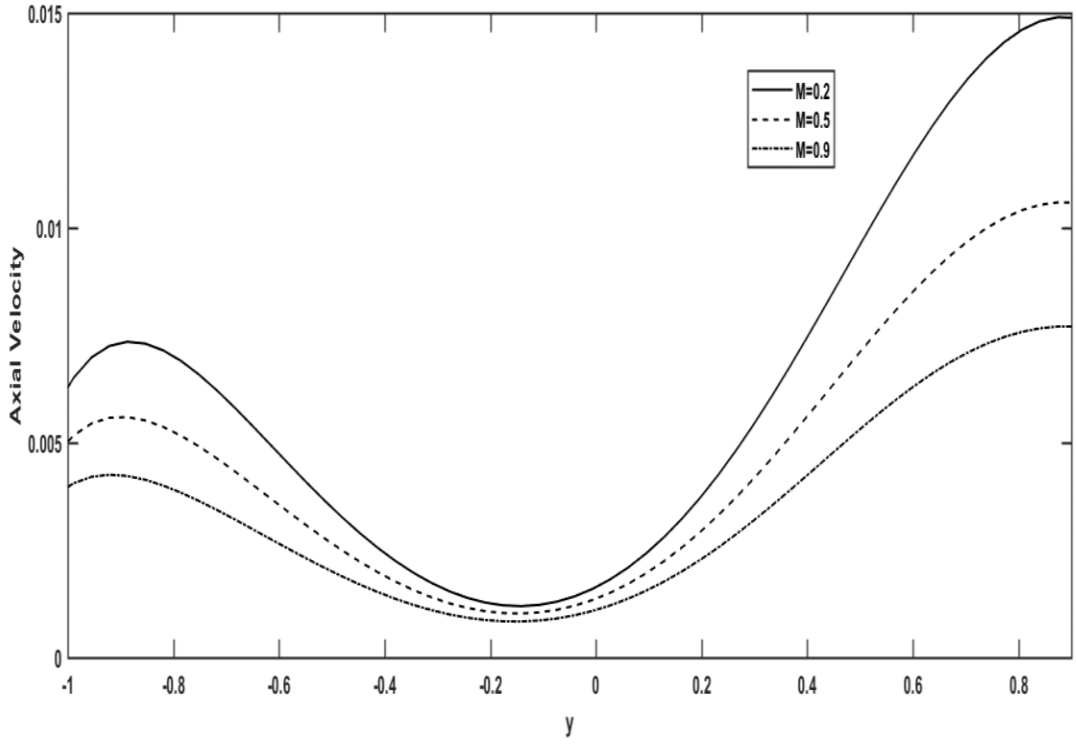

Fig. 3: Axial velocity for M for $\alpha = 0.5,\ Pr = 7.56,\ Ma = 0.3, d = 1.5, Gr = 5$.

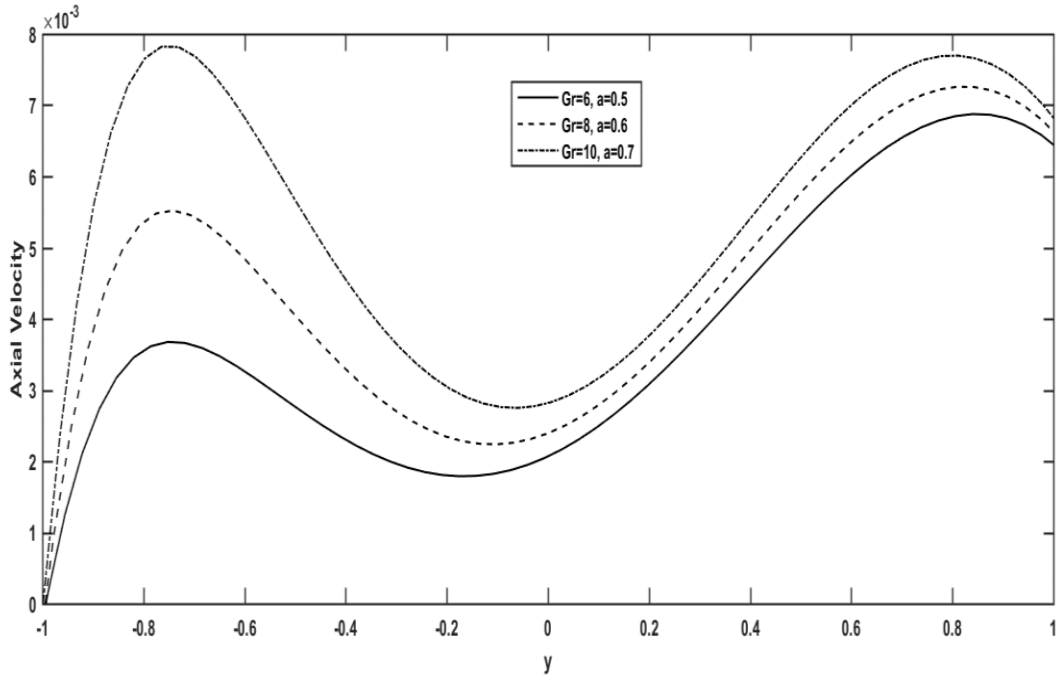

Fig. 4: Axial velocity for a for $d = 1.5,\ Pr = 7.56, \chi = 0.5, M = 0.9\ Ma = 0.3$.

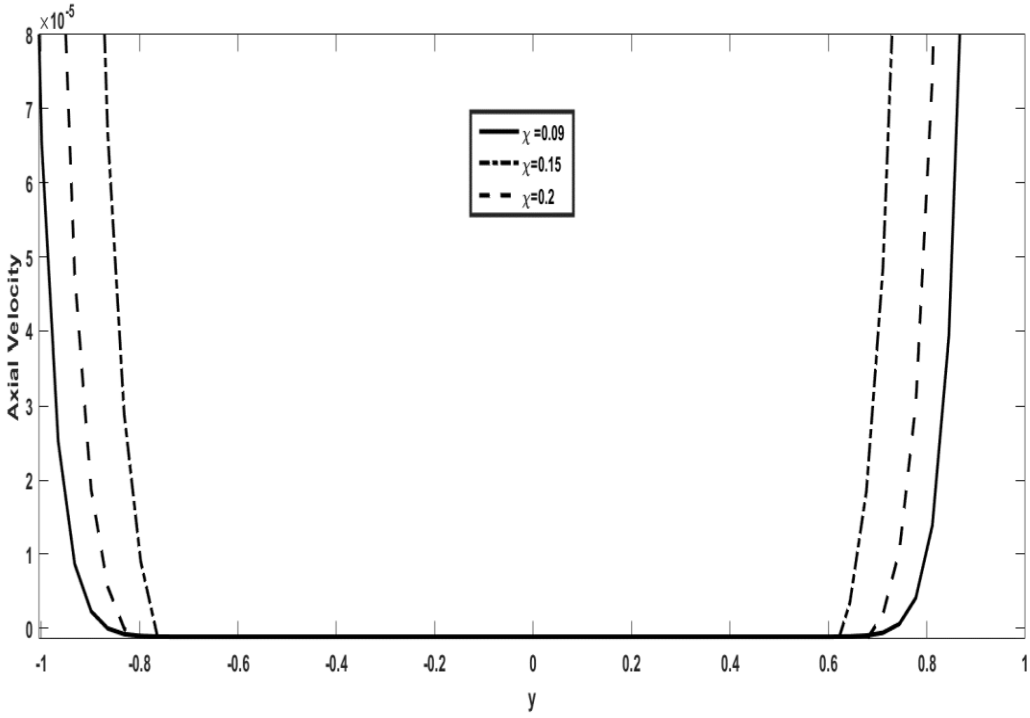

Fig. 5: Axial velocity for χ for $\alpha = 0.5,\ Pr = 7.56,\ Ma = 0.3, \epsilon = 0.5, Gr = 7.$

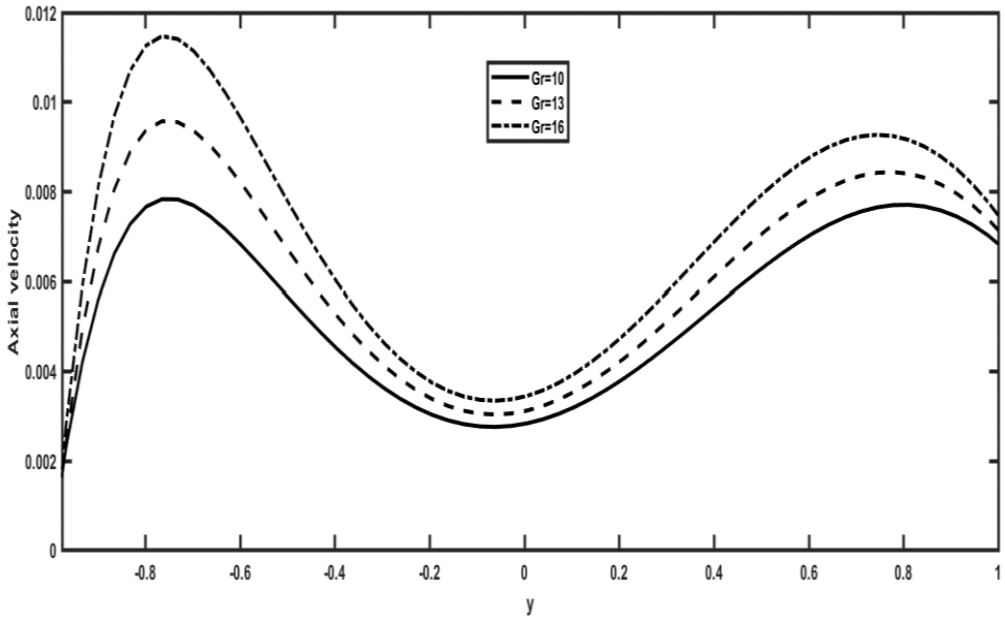

Fig. 6: Axial velocity for Gr for $\alpha = 0.5, \epsilon = 0.5,\ Pr = 7.56, M = 0.9,\ Ma = 0.3.$

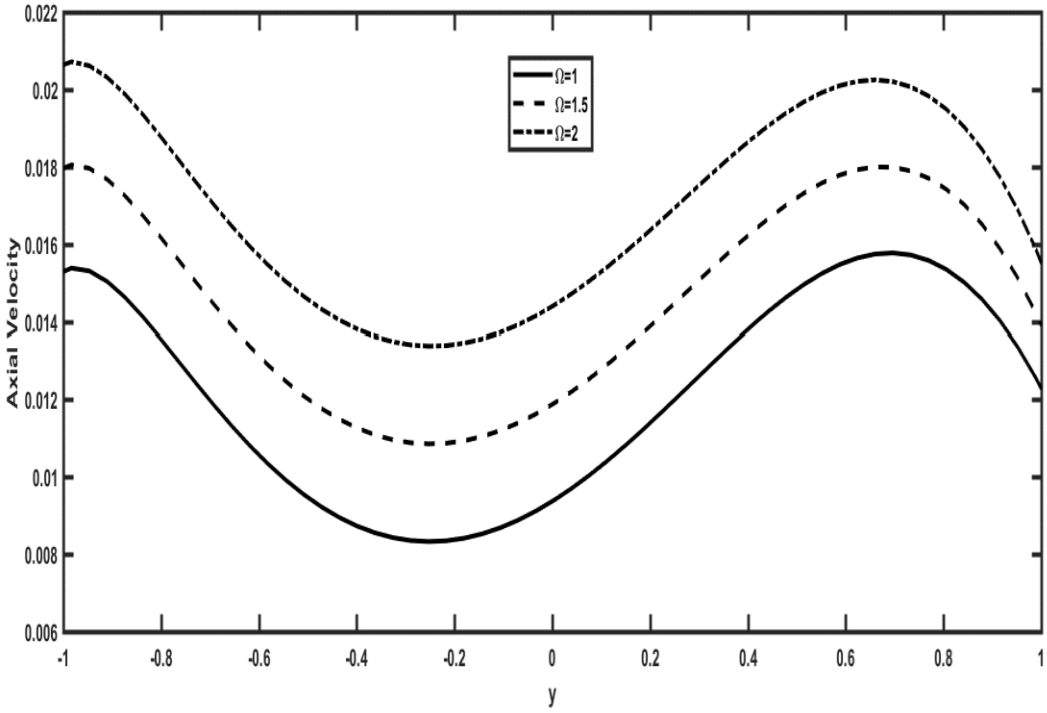

Fig. 7: Axial velocity for source Ω for $Gr = 16,\ \alpha = 0.5, \chi = 0.5,\ Pr = 7.56, Ma = 0.3$.

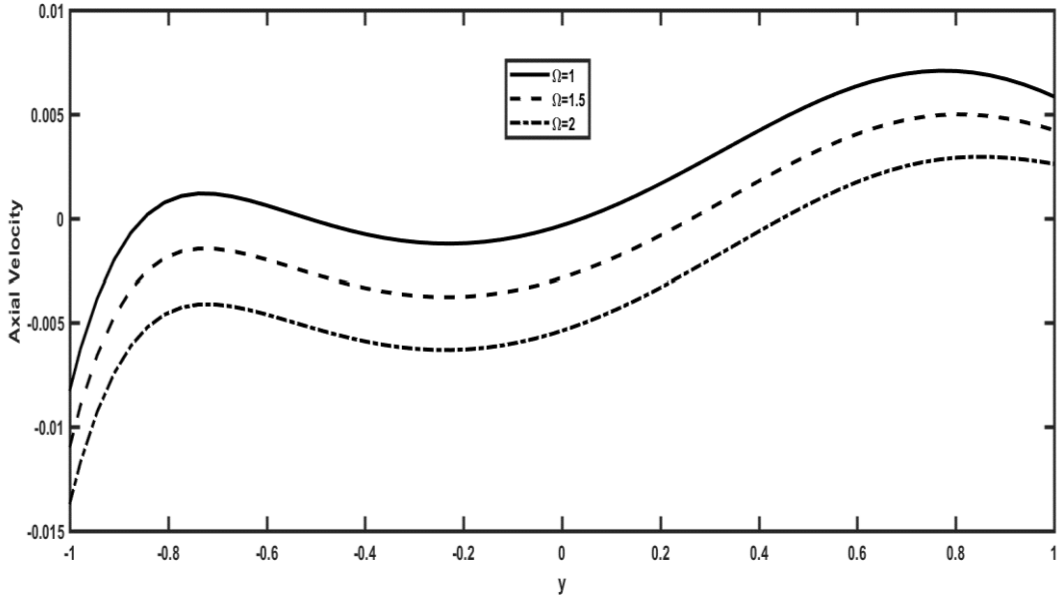

Fig. 8: Axial velocity for sink Ω for $\alpha = 0.5, \chi = 0.5, Gr = 16,\ Pr = 7.56,\ Ma = 0.3$.

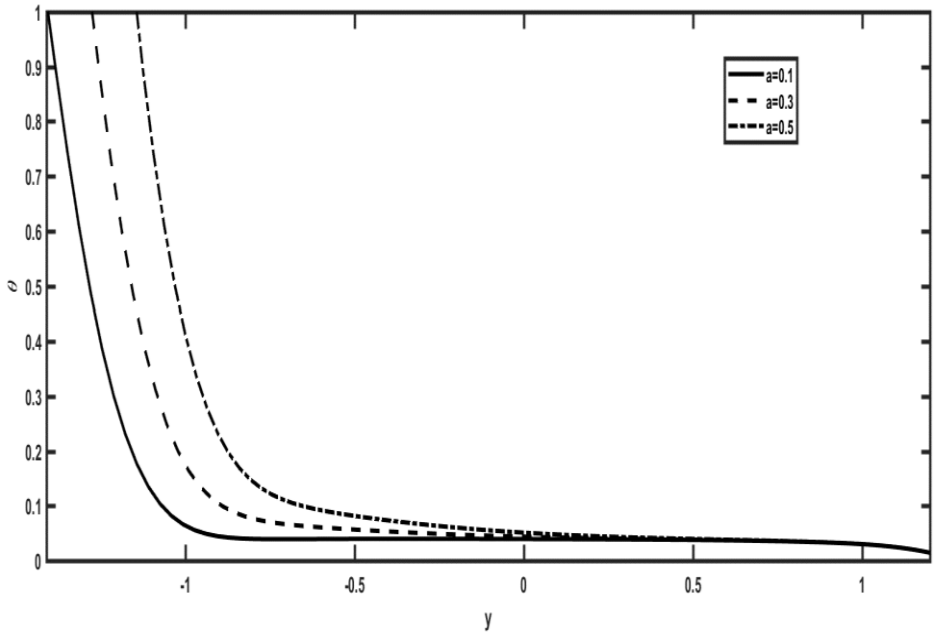

Fig. 9: Temperature with a for

$$\alpha = 0.5, \epsilon = 0.5,\ Ma = 0.1, \phi = \frac{\pi}{4}, R = 50, d = 1.5, Pr = 7.56,.$$

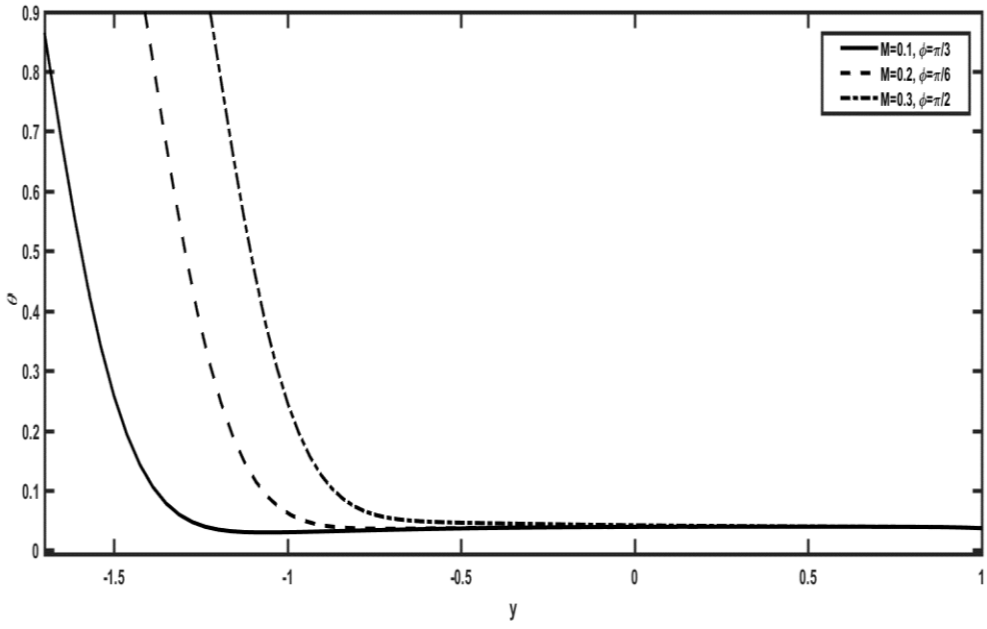

Fig. 10: Temperature for M for

$$\alpha = 0.5, \phi = \frac{\pi}{4}, \epsilon = 0.5, d = 1.5, Ma = 0.1, \chi = 0.5, R = 50, Pr = 7.56.$$

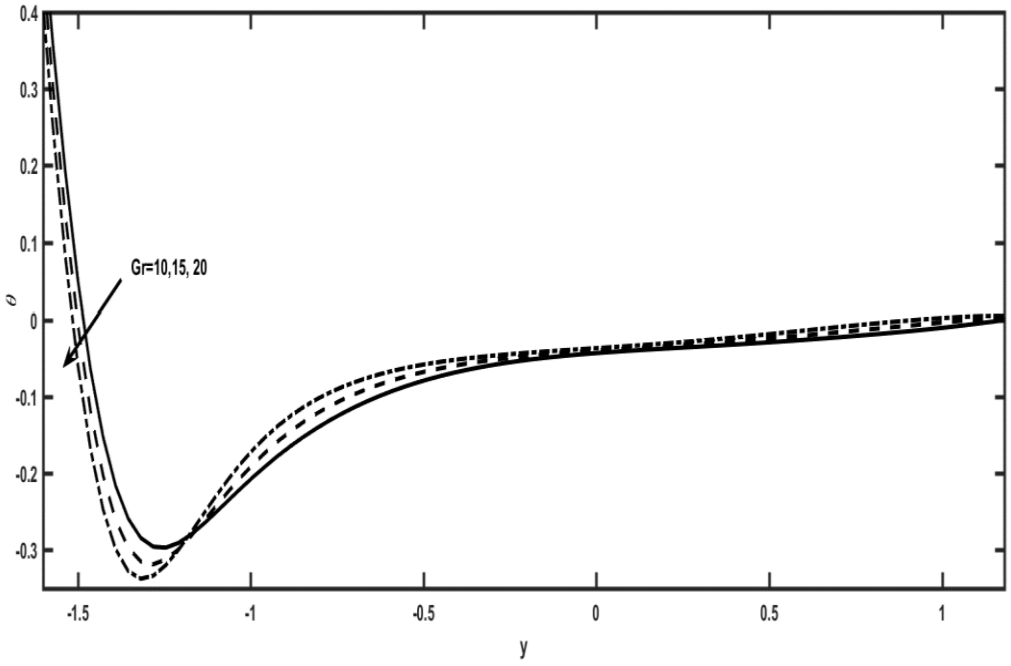

Fig. 11: Temperature for Gr for

$\alpha = 0.5, Ma = 0.5, \epsilon = 0.5, M = 0.5\ , \phi = \frac{\pi}{4}, d = 1.5, \chi = 0.5, R = 50, , Pr = 7.56$.

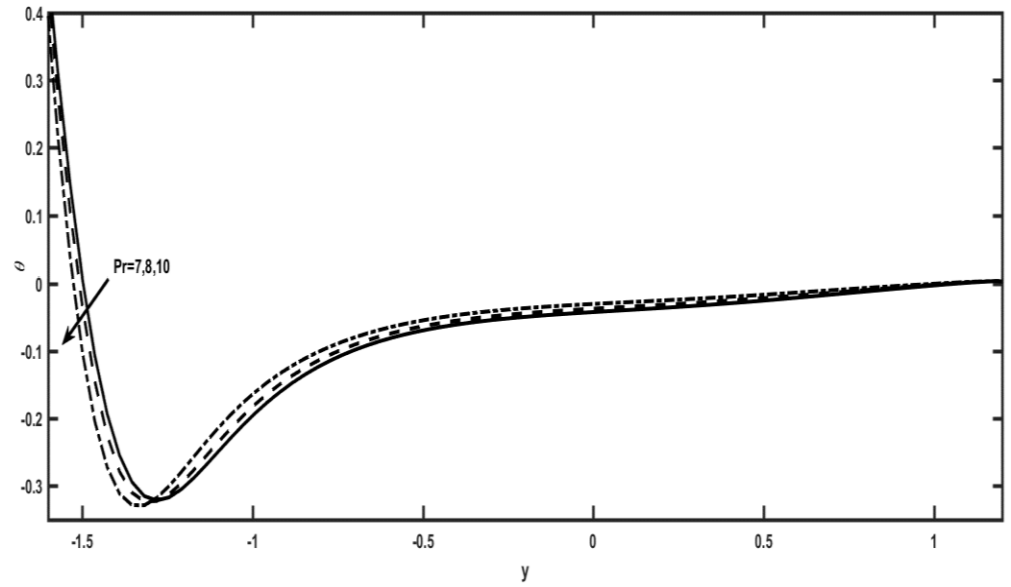

Fig. 12: Temperature for Pr for

$\alpha = 0.5, \phi = \frac{\pi}{4}, \epsilon = 0.5, Ma = 0.5, \chi = 0.5, d = 1.5, M = 0.5, R = 50,\ Gr = 16$.

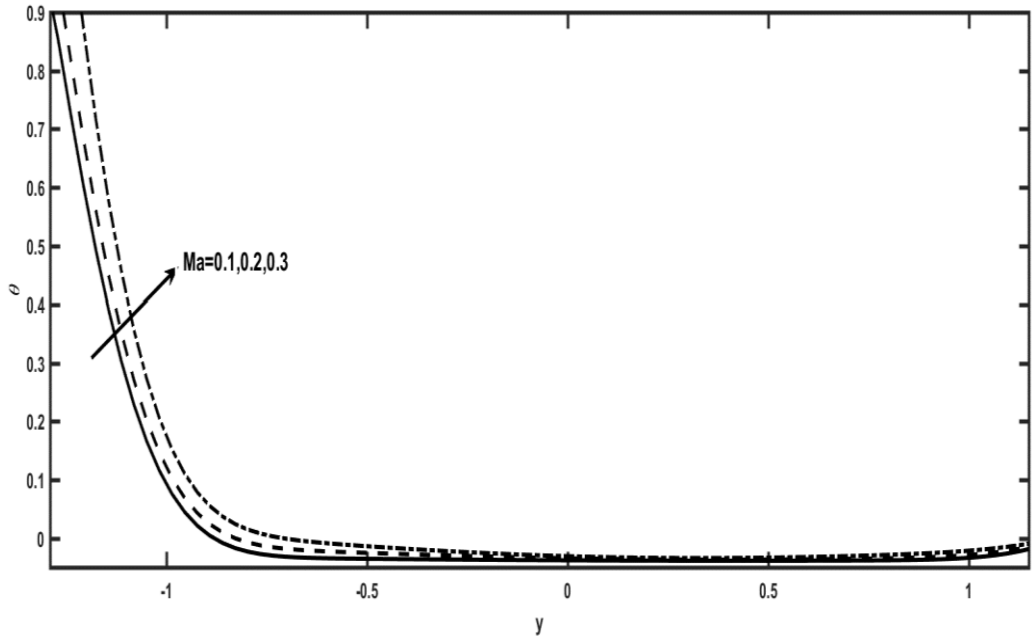

Fig. 13: Temperature for Ma for

$\phi = \frac{\pi}{2}, Pr = 7.56, \epsilon = 0.5,\ \alpha = 0.5, \chi = 0.5, R = 50, M = 0.5,\ d = 1.5, Gr = 16$.

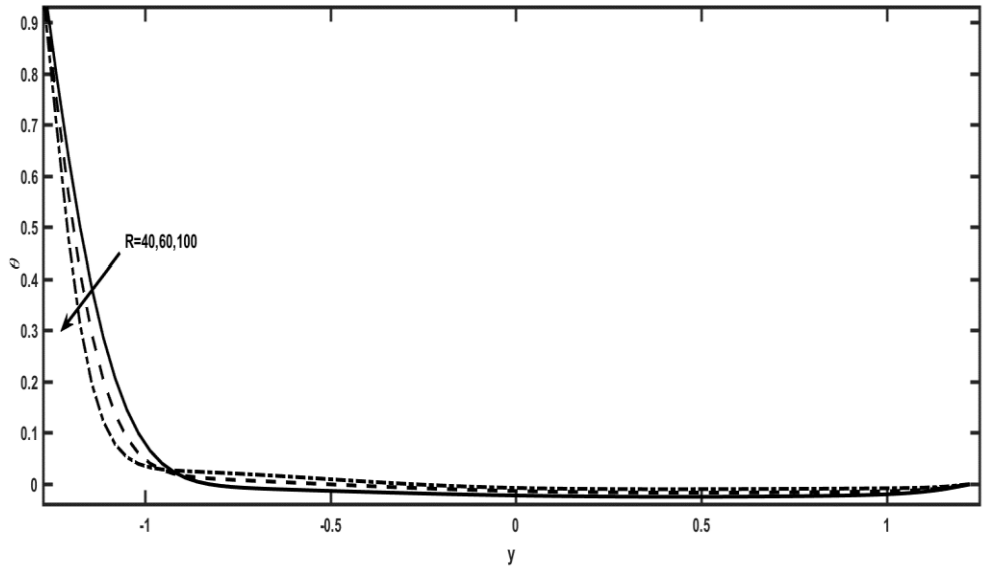

Fig. 14: Temperature for R for

$d = 1.5, \epsilon = 0.5, \alpha = 0.5, Pr = 7.56, , \chi = 0.5, Gr = 16, M = 0.5, \phi = \frac{\pi}{2}, Ma = 0.2$.

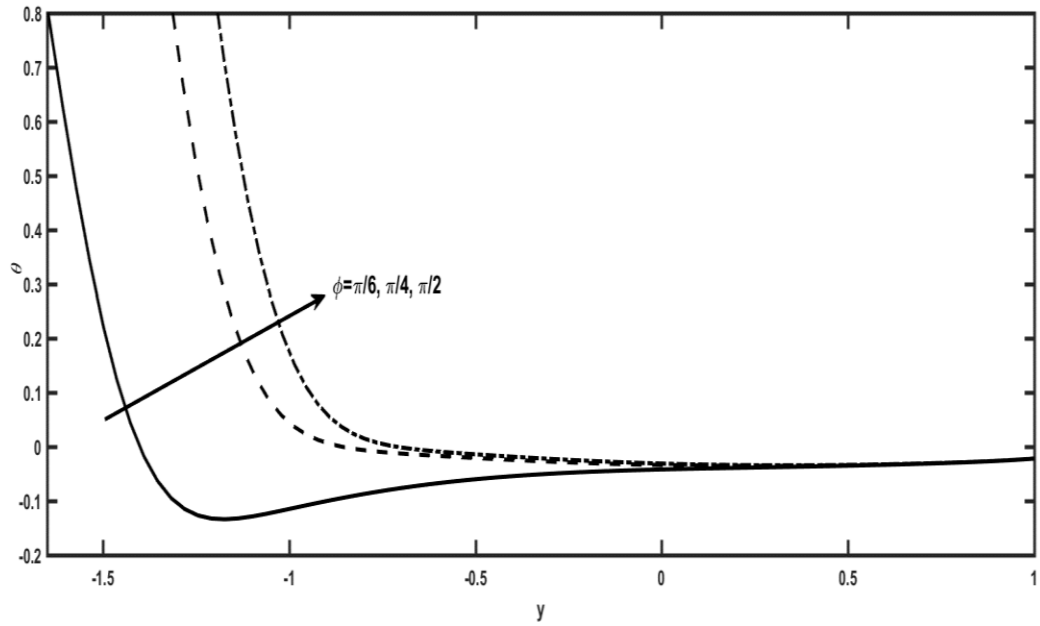

Fig. 15: Temperature for ϕ for

$\alpha = 0.5, d = 1.5, \epsilon = 0.5, \chi = 0.5, Pr = 7.56, M = 0.5, Ma = 0.2,\ Gr = 16, R = 50.$

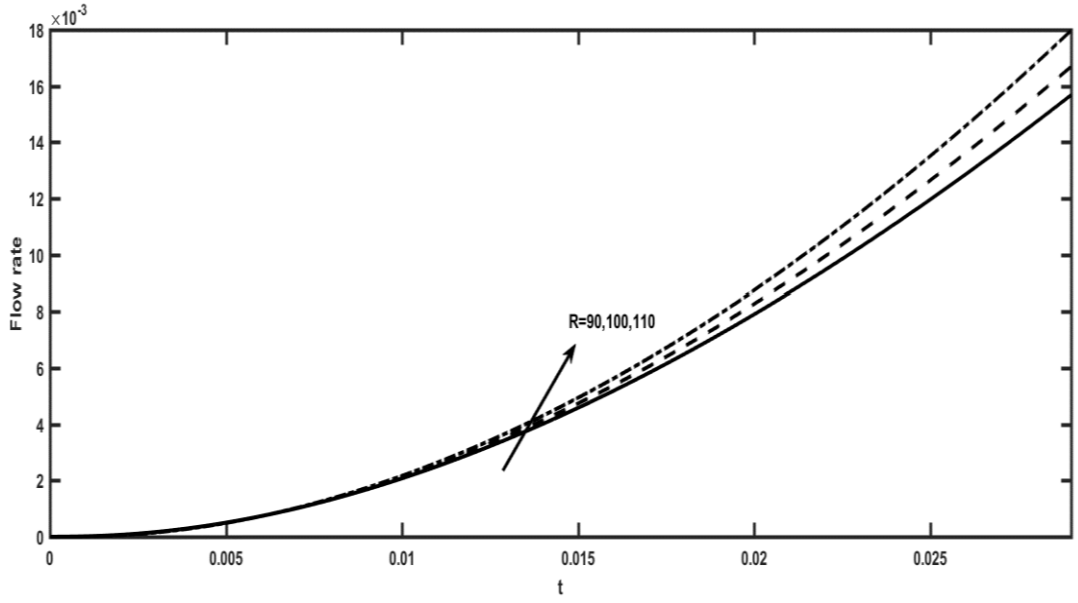

Fig. 16: Flow Rate for R for

$\epsilon = 0.4, \alpha = 0.5,\ \phi = \frac{\pi}{6}, d = 1.5, \chi = 0.5, M = 0.5, Pr = 11, Ma = 0.59,\ Gr = 16.$

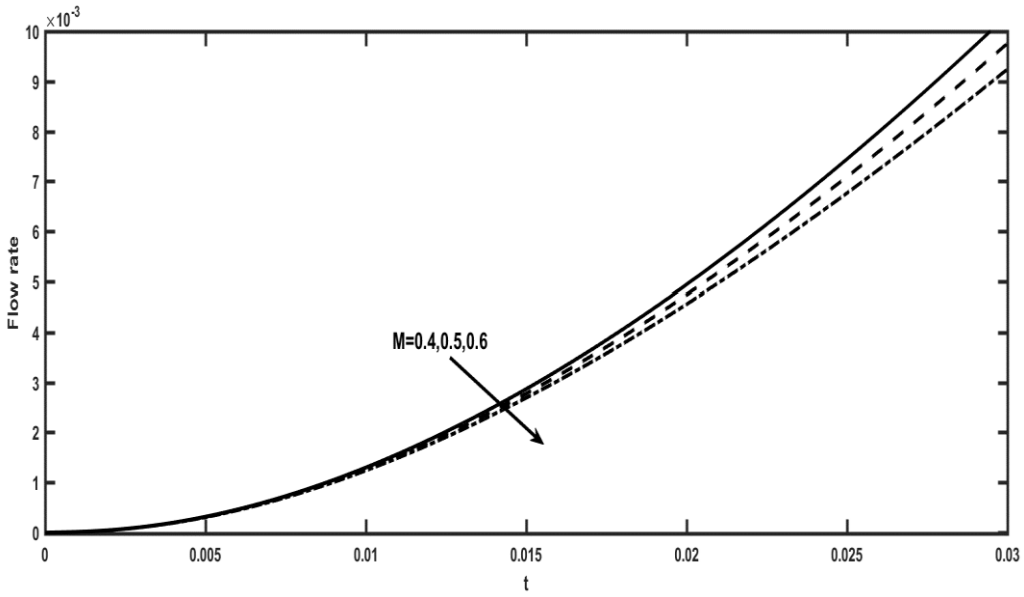

Fig. 17: Flow Rate for M for

$$d = 1.5, \epsilon = 0.4, \alpha = 0.5, \chi = 0.45, \phi = \frac{\pi}{6}, R = 110, Ma = 0.59, Pr = 11, Gr = 16 .$$

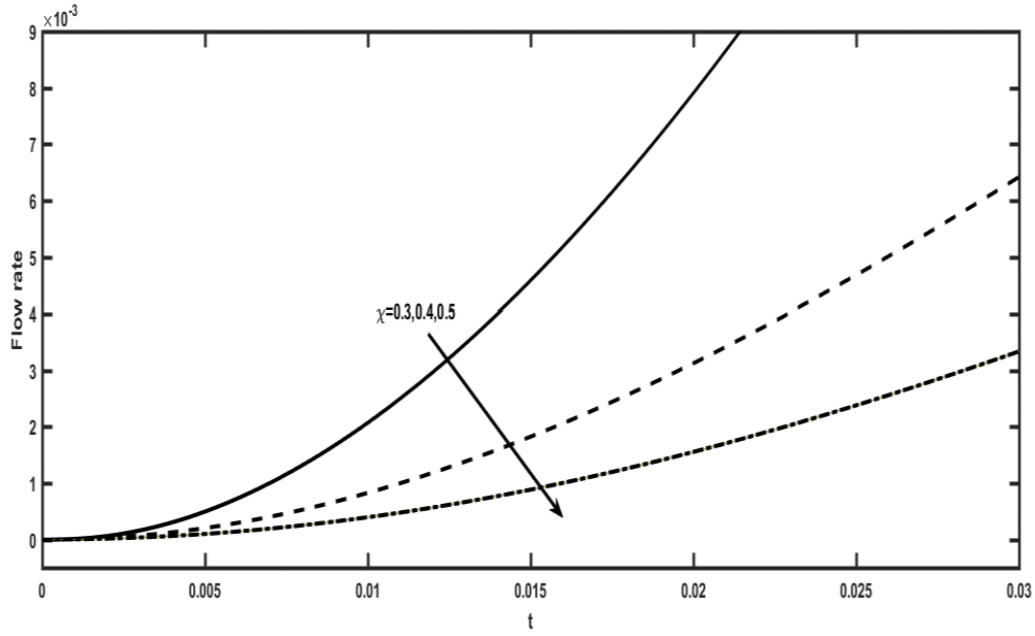

Fig. 18: Flow Rate for χ for

$$\alpha = 0.5, \epsilon = 0.4, d = 1.5, M = 0.5, R = 110, Ma = 0.59, Pr = 11, Gr = 16, \phi = \frac{\pi}{6} .$$

- Fluid velocity is enhanced in the source case while showing the reverse behavior in the sink case.
- The analysis of temperature dispensation shows an oscillating behavior for buoyancy forces and inertial forces.
- Thermal dispensation shows an increasing behavior for Mach number.
- Temperature is enhanced when the magnetic number increases. It is just due to the retarding force.
- Flow rate drops when magnetic number and compressibility parameter increases.

- Flow rate shows incremental behavior when the inertial forces are dominant.

References

[1] T. W. Latham, *Fluid motions in a peristaltic pump*, Thesis, Massachusetts Institute of Technology, 1966.

[2] A. H. Shapiro, M. Y. Jaffrin, S. L. Weinberg, Peristaltic pumping with long wavelengths at low Reynolds number, *Journal of Fluid Mechanics*, Vol. 37, No. 4, pp. 799-825, 1969.

[3] E. Elshehawey, A. Sobh, E. Elbarbary, Peristaltic Motion of a Generalized Newtonian Fluid Through a Porous Medium, *Journal of The Physical Society of Japan - J PHYS SOC JPN*, Vol. 69, pp. 401-407, 02/15, 2000.

[4] A. M. Siddiqui, W. H. Schwarz, Peristaltic flow of a second-order fluid in tubes, *Journal of Non-Newtonian Fluid Mechanics*, Vol. 53, pp. 257-284, 1994/07/01/, 1994.

[5] H. Vaidya, O. Makinde, R. Choudhari, K. Prasad, S. Khan, K. Vajravelu, Peristaltic flow of non-Newtonian fluid through an inclined complaint nonlinear tube: application to chyme transport in the gastrointestinal tract, *European Physical Journal Plus*, Vol. 135, pp. 934, 11/24, 2020.

[6] T. Hayat, S. Hina, S. Asghar, S. Obaidat, Peristaltic flow of Maxwell fluid in an asymmetric channel with wall properties, *Int. J. Phys. Sci.*, Vol. 7, pp. 2145-2155, 01/01, 2012.

[7] G. I. Taylor, Analysis of the swimming of microscopic organisms, *Proceedings of the Royal Society of London. Series A. Mathematical and Physical Sciences*, Vol. 209, No. 1099, pp. 447-461, 1951.

[8] O. Eytan, D. Elad, Analysis of intra-uterine fluid motion induced by uterine contractions, *Bulletin of Mathematical Biology*, Vol. 61, No. 2, pp. 221-238, 1999.

[9] N. Ali, K. Ullah, H. Kazmi, Bifurcation analysis for a two-dimensional peristaltic driven flow of power-law fluid in asymmetric channel, *Physics of Fluids*, Vol. 32, pp. 073104, 07/01, 2020.

[10] M. Kothandapani, J. Prakash, V. Pushparaj, Nonlinear peristaltic motion of a Johnson–Segalman fluid in a tapered asymmetric channel, *Alexandria Engineering Journal*, Vol. 55, No. 2, pp. 1607-1618, 2016/06/01/, 2016.

[11] R. Rafaqat, A. A. Khan, Effects of magnetic field and porosity on compressible flow in an asymmetric channel, *International Journal of Modern Physics B*, Vol. 38, No. 19, pp. 2450246, 2024.

[12] F. H. Harlow, J. E. Welch, Numerical Calculation of Time-Dependent Viscous Incompressible Flow of Fluid with Free Surface, *The Physics of Fluids*, Vol. 8, No. 12, pp. 2182-2189, 1965.

[13] A. Abbasi, A. Zaman, S. Arooj, M. Ijaz Khan, S. U. Khan, W. Farooq, T. Muhammad, A bioconvection model for viscoelastic nanofluid confined by tapered asymmetric channel: implicit finite difference simulations, *J Biol Phys*, Vol. 47, No. 4, pp. 499-520, Dec, 2021. eng

[14] T. Hayat, K. Muhammad, S. Momani, Melting heat and viscous dissipation in flow of hybrid nanomaterial: a numerical study via finite difference method, *Journal of Thermal Analysis and Calorimetry*, pp. 1-9, 2022.

[15] S. Reza-E-Rabbi, S. M. Arifuzzaman, T. Sarkar, M. S. Khan, S. F. Ahmmed, Explicit finite difference analysis of an unsteady MHD flow of a chemically reacting Casson fluid past a stretching sheet with Brownian motion and thermophoresis effects, *Journal of King Saud University - Science*, Vol. 32, No. 1, pp. 690-701, 2020/01/01/, 2020.

[16] A. R. A. Khaled, K. Vafai, Heat transfer enhancement through control of thermal dispersion effects, *International Journal of Heat and Mass Transfer*, Vol. 48, No. 11, pp. 2172-2185, 2005/05/01/, 2005.

[17] M. A. Sheremet, M. M. Rashidi, Thermal convection of nano-liquid in an electronic cabinet with finned heat sink and heat generating element, *Alexandria Engineering Journal*, Vol. 60, No. 3, pp. 2769-2778, 2021/06/01/, 2021.

[18] M. M. Bhatti, A. Zeeshan, N. Ijaz, O. Bég, A. Kadir, Mathematical modelling of nonlinear thermal radiation effects on EMHD peristaltic pumping of viscoelastic dusty fluid through a porous medium duct, *Engineering Science and Technology, an International Journal*, Vol. 20, 11/01, 2016.

[19] T. Thumma, S. Mishra, M. A. Abbas, M. M. Bhatti, S. I. Abdelsalam, Three-dimensional nanofluid stirring with non-uniform heat source/sink through an elongated sheet, *Applied Mathematics and Computation*, Vol. 421, pp. 126927, 2022.

[20] S. Baragh, H. Shokouhmand, S. Mousavi Ajarostaghi, M. Nikian, An experimental investigation on forced convection heat transfer of single phase flow in a channel with different arrangements of porous media, *International Journal of Thermal Sciences*, Vol. 134, pp. 370-379, 08/23, 2018.

[21] H. Shokouhmand, F. Sangtarash, The effect of flexible tube vibration on pressure drop and heat transfer in heat exchangers considering viscous dissipation effects, *Heat and Mass Transfer*, Vol. 44, pp. 1435-1445, 01/10, 2008.

[22] N. Ranjit, G. Shit, A. Sinha, Transportation of ionic liquids in a porous micro-channel induced by peristaltic wave with Joule heating and wall-slip conditions, *Chemical Engineering Science*, Vol. 171, pp. 545-557, 2017.

[23] P. Gholamalipour, M. Siavashi, M. H. Doranehgard, Eccentricity effects of heat source inside a porous annulus on the natural convection heat transfer and entropy generation of Cu-water nanofluid, *International Communications in Heat and Mass Transfer*, Vol. 109, pp. 104367, 2019/12/01/, 2019.

[24] M. Turkyilmazoglu, An analytical treatment for the exact solutions of MHD flow and heat over two–three dimensional deforming bodies, *International Journal of Heat and Mass Transfer*, Vol. 90, pp. 781-789, 2015/11/01/, 2015.

[25] L. Zhang, M. M. Bhatti, M. Marin, K. S. Mekheimer, Entropy Analysis on the Blood Flow through Anisotropically Tapered Arteries Filled with Magnetic Zinc-Oxide (ZnO) Nanoparticles, *Entropy*, Vol. 22, No. 10, pp. 1070, 2020.

[26] N. Gibanov, M. Sheremet, H. Öztop, K. Al-Salem, MHD natural convection and entropy generation in an open cavity having different horizontal porous blocks saturated with a ferrofluid, *Journal of Magnetism and Magnetic Materials*, Vol. 452, 12/01, 2017.

[27] A. Aarts, G. Ooms, Net flow of compressible viscous liquids induced by travelling waves in porous media, *Journal of engineering mathematics*, Vol. 34, pp. 435-450, 1998.

[28] K. Mekheimer, S. Komy, S. Abdelsalam, Simultaneous effects of magnetic field and space porosity on compressible Maxwell fluid transport induced by a surface acoustic wave in a microchannel, *Chinese Physics B*, Vol. 22, pp. 124702, 12/01, 2013.